ICSE2012 – 6th International Conference on Scar and Erosion
Paris, France, 29-31 August 2012

Numerical analysis of embankment erosion caused by overflow using shallow water equations

K. Fujisawa*, A. Murakami** , S. Nishimura*& T. Shuku*
*Okayama University, Japan
**Kyoto University, Japan

Background

Overflow and piping are the primary causes of failures of embankments such as dams, levees and irrigation ponds

1. **Overflow** 70 to 80% of levee failures have been caused by overflow. About 50% of dam breaks have been caused by overflow.

2. **Piping**

   40% of causes of dam breaks

3. Slide

   a few percents

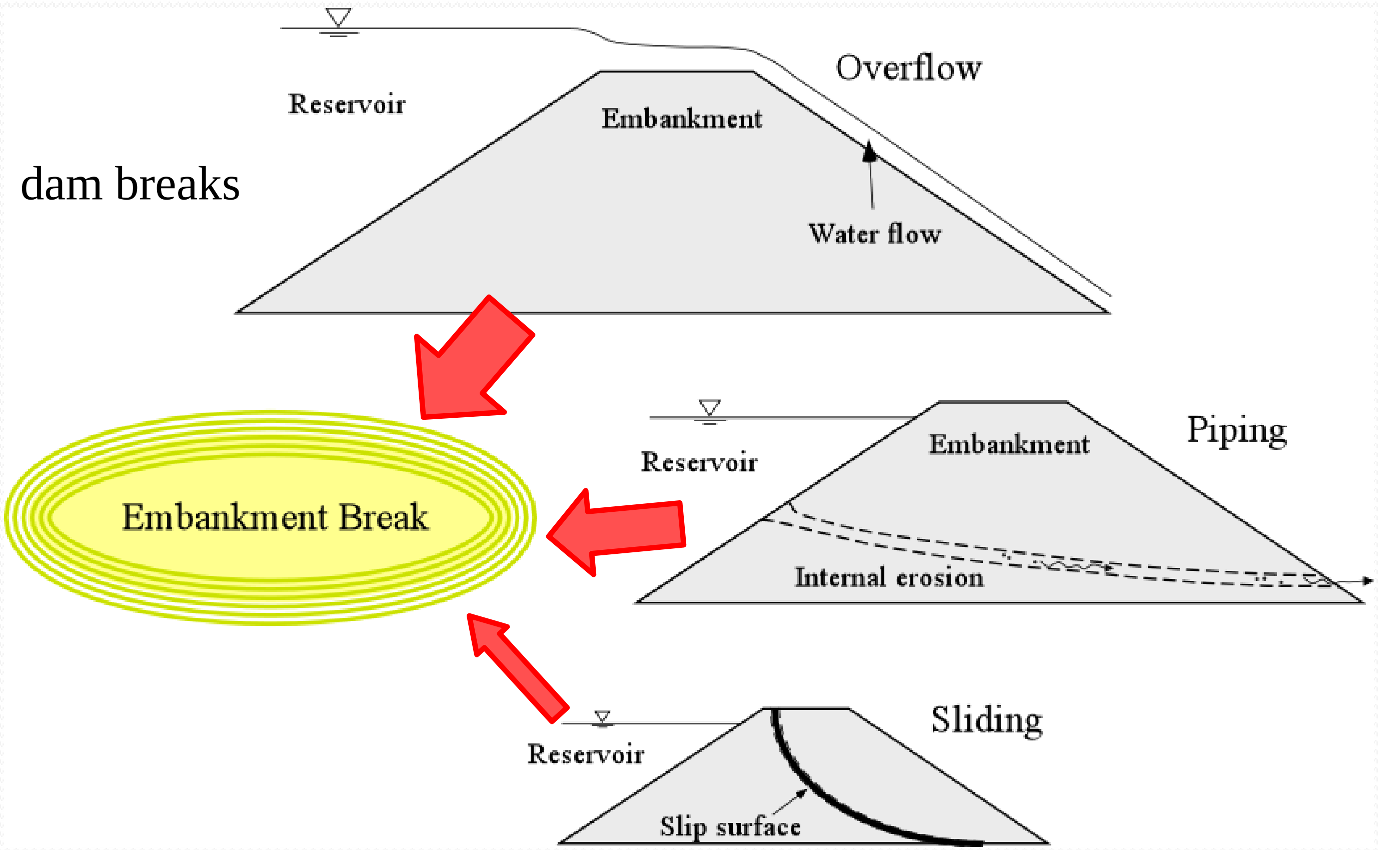

Cases of irrigation ponds

Irrigation ponds which failed due to overflow in 2004, Awaji Island, Japan

Plunge pool

Loss of vegetation

Case of a levee

A levee suffering overflow
in 2004, Fukui pref., Japan

Previous studies

Visser (1998) and Coleman et al. (2002) investigated the breaching process of cohesionless embankments during overtopping failure

Zhu (2006) focused his investigation on the failure process of cohesive embankments.

Hanson et al. (2005) conducted large-scale overflow-embankment tests using silty sand and a clayey material, and Hanson et al. (2011) integrated the material properties for embankment breach. They have intensiely been working on the headcut advance, too.

Numerical and theoretical studies on this topic have been reported as well .(e.g., Zerrouk & Marche 2004; Wang & Bowles 2006; Wang & Bowles 2007; Faeh 2007; Fujisawa et al. 2009)

When does the headcut appear ?

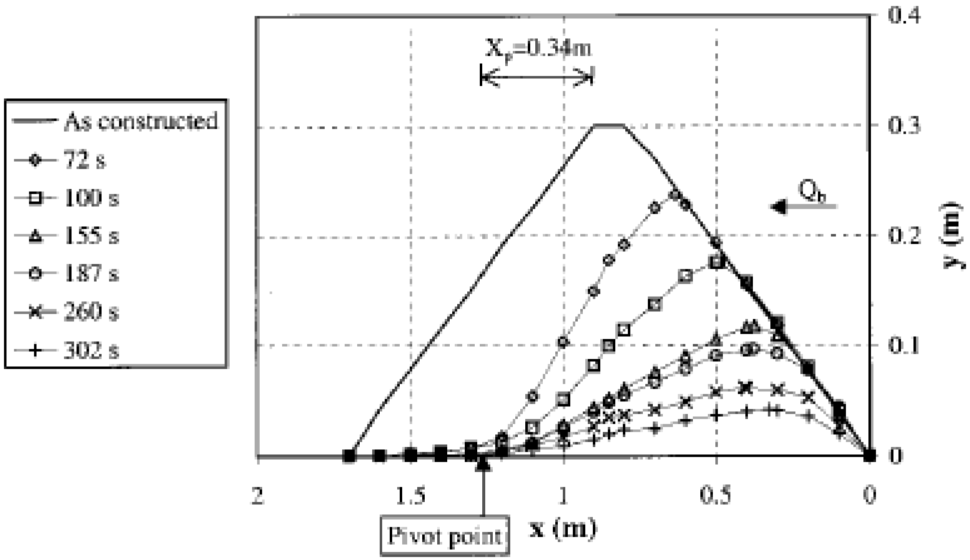

Cohesionless material

Coleman et al. (2002).
Overtopping Breaching of Noncohesive Homogeneous Embankment, *Journal of Hydraulic Engineering*, ASCE, Vol.128

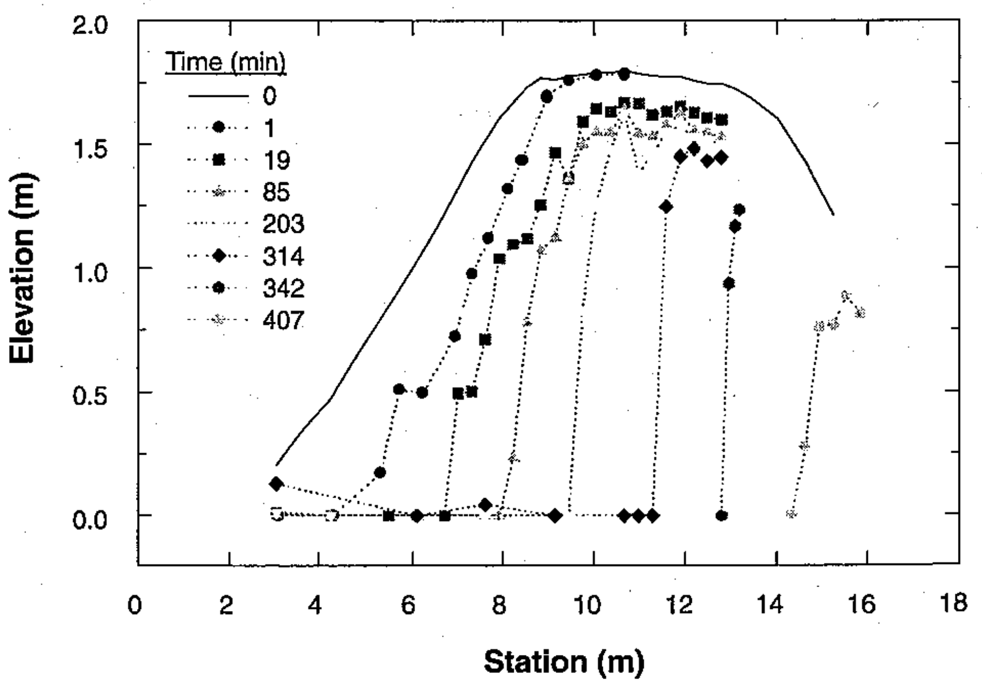

Cohesive material

Hanson et al. (2005).
Physical Modeling of Overtopping Erosion and Breach Formation of Cohesive Embankments, *Transactions of the ASAE*, Vol.48

Hydraulics – Where does the erosion starts and develop? -

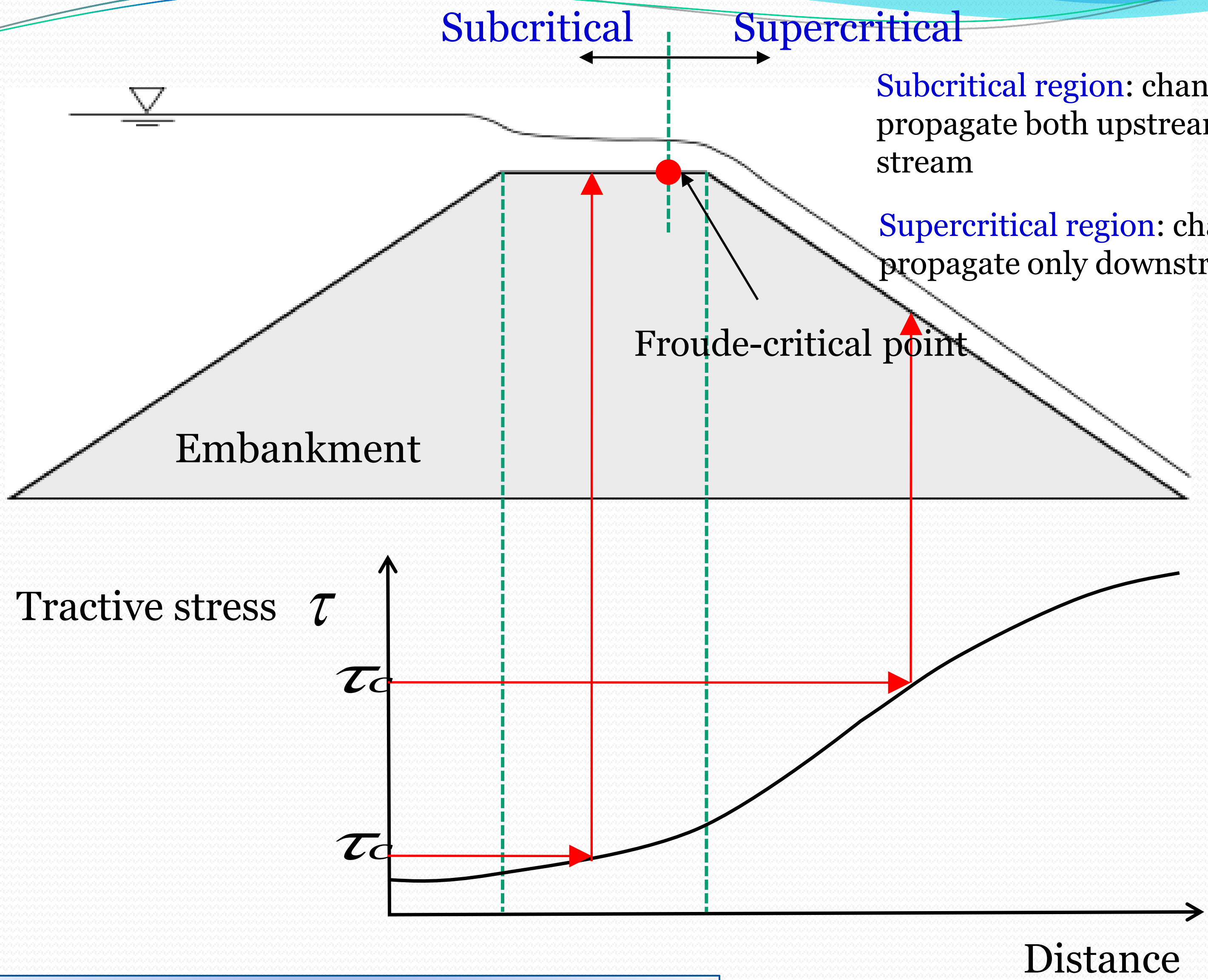

Subcritical region: changes in flow can propagate both upstream and down stream

Supercritical region: changes in flow propagate only downstream

Where the friction stress reaches the critical stress and the erosion start

Erosion on supercritical region

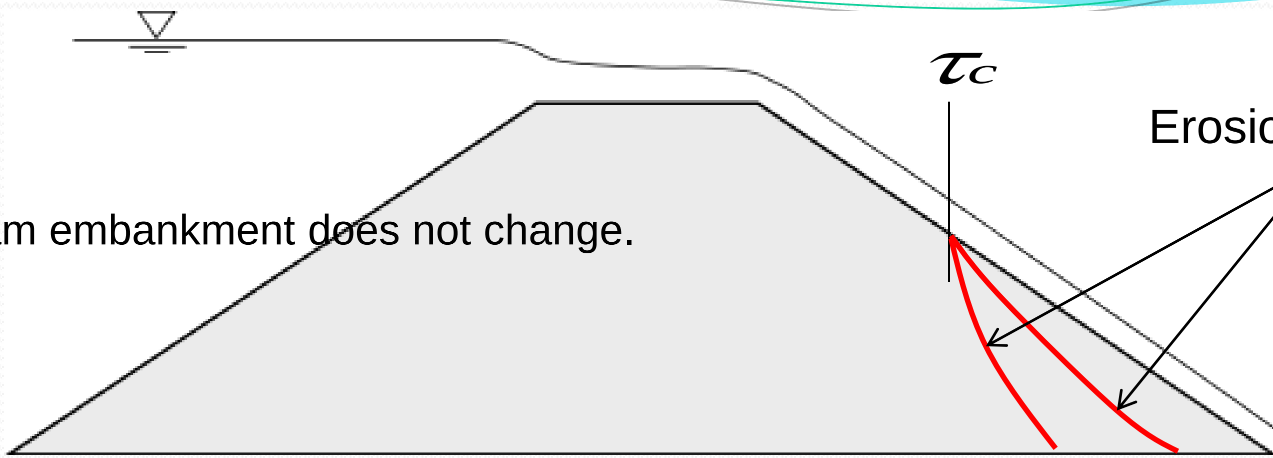

The upstream embankment does not change.

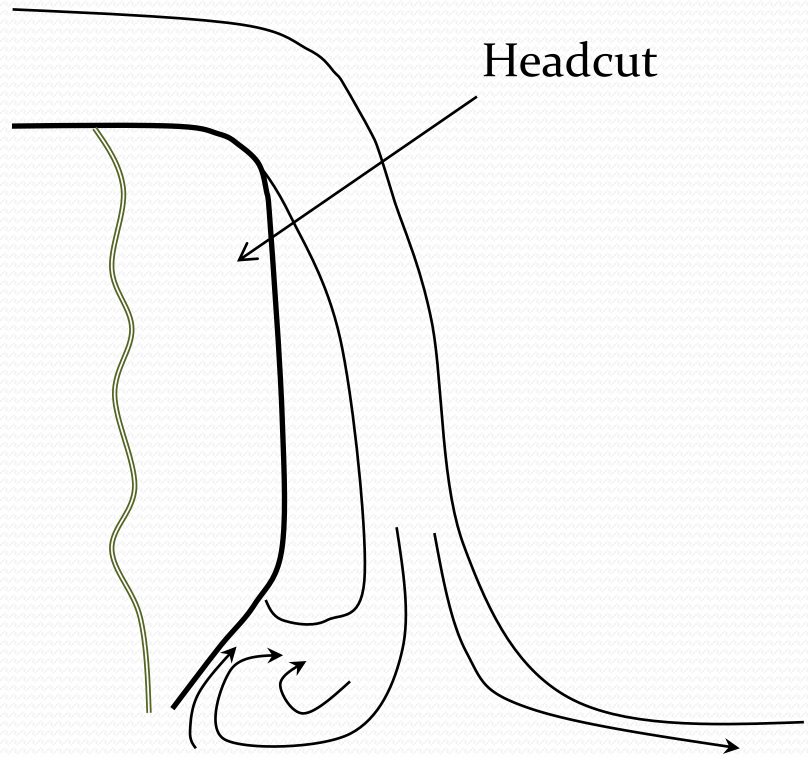

Erosion on subcritical region

The entire profile of the embankment is changing

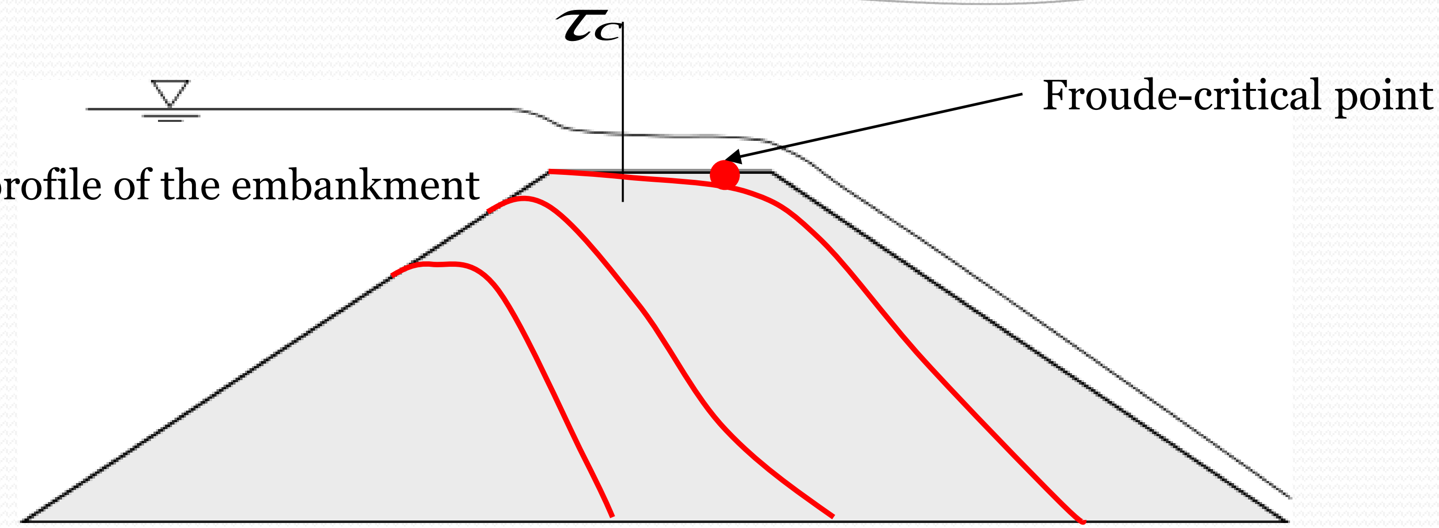

Governing equations

2 D shallow water equations

$$\frac{\partial \boldsymbol{U}}{\partial t}+\frac{\partial \boldsymbol{F}}{\partial x}+\frac{\partial \boldsymbol{G}}{\partial y}=\boldsymbol{S}$$

$$\boldsymbol{U}=\begin{pmatrix} h \\ uh \\ vh \end{pmatrix} \quad \boldsymbol{F}=\begin{pmatrix} uh \\ u^2h+gh^2/2 \\ uvh \end{pmatrix} \quad \boldsymbol{G}=\begin{pmatrix} vh \\ uvh \\ v^2h+gh^2/2 \end{pmatrix}$$

$$\boldsymbol{S}=\begin{pmatrix} 0 \\ \boxed{-gh(\partial z/\partial x}+S_{fx}) \\ \boxed{-gh(\partial z/\partial y}+S_{fy}) \end{pmatrix}$$

Finite Volume Method

Temporal change of erosion surface

$$\boxed{\frac{\partial z}{\partial t}}=-\frac{E(\boldsymbol{U})}{1-\lambda_p}$$

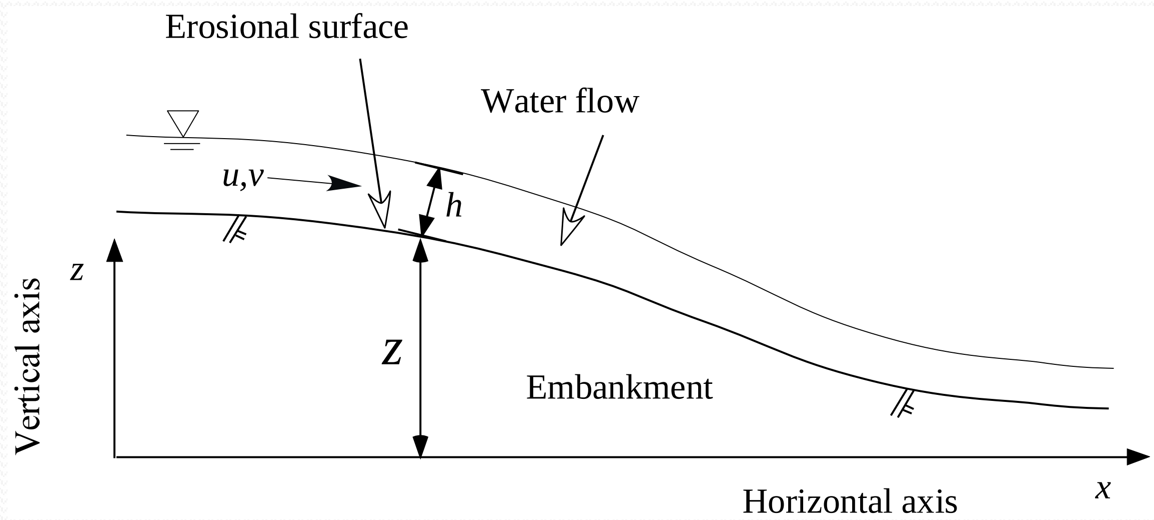

Erosion of soils

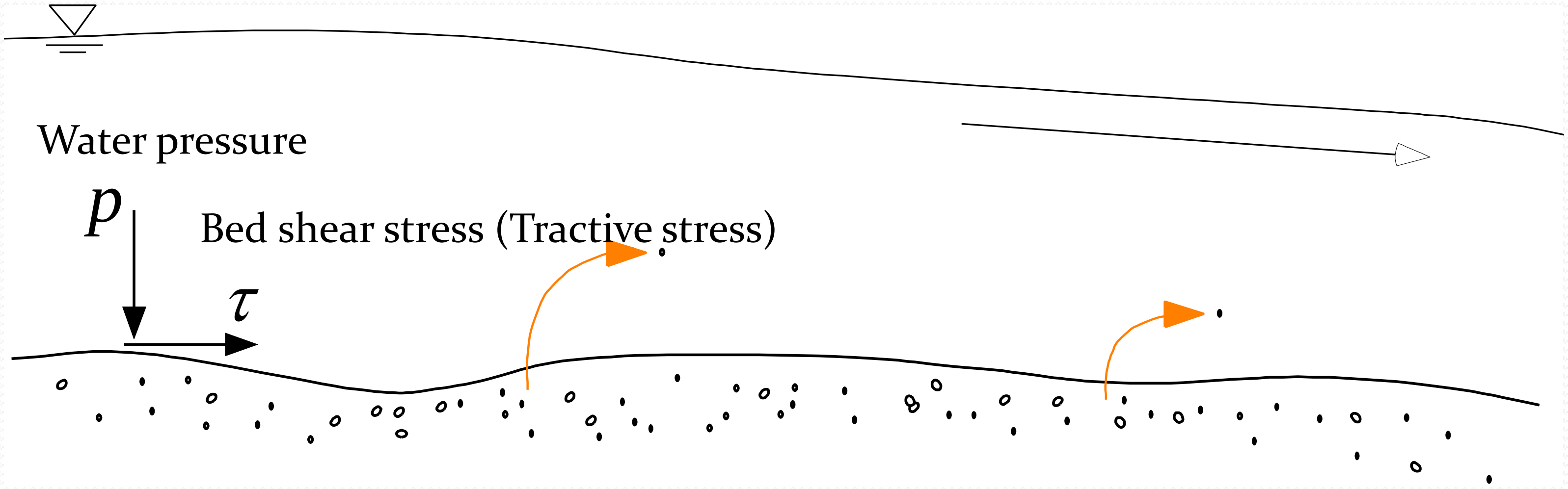

Erosion rate E = Volume of soils eroded from unit surface area during unit time

$$E = \alpha(\tau - \tau_c)^{\gamma}$$

Erosion rate: E

Applied shear stress: τ

Material constants: α γ

Critical shear stress: τ_c

Finite Volume Approach

Area integral

$$\int_{A_i} \frac{\partial \boldsymbol{U}}{\partial t} + \frac{\partial \boldsymbol{F}}{\partial x} + \frac{\partial \boldsymbol{G}}{\partial y}\, dA = \int_{A_i} \boldsymbol{S}\, dA$$

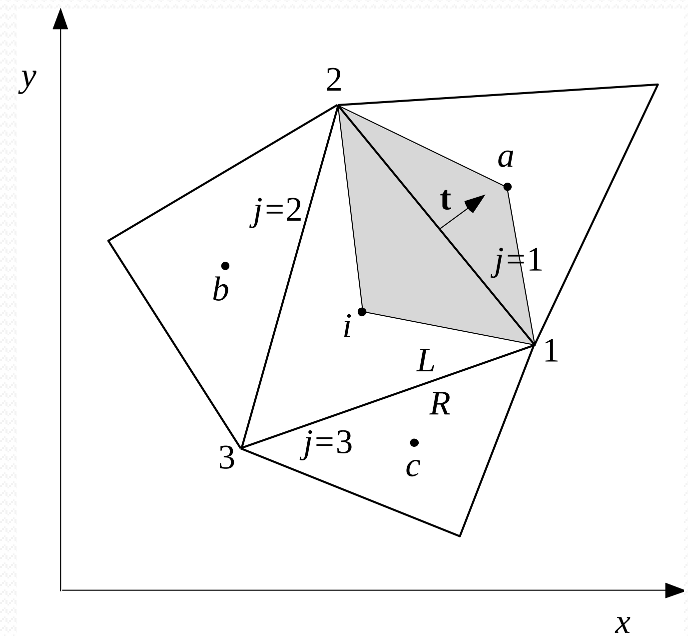

Divergence theorem of Gauss

$$\frac{d}{dt}\int_{A_i} \boldsymbol{U} dA = -\oint_{\Gamma} \boldsymbol{E}^* d\Gamma + \int_{A_i} \boldsymbol{S}\, dA$$

Intercell normal flux $\boldsymbol{E}^* = \boldsymbol{F} t_x + \boldsymbol{G} t_y$

Finite volume approximation for each cell

$$\frac{d\boldsymbol{U}}{dt} = \frac{1}{A_i}\sum_j \boldsymbol{E}^* \Delta\Gamma_{ij} + \boldsymbol{S}$$

A_i : Area of ith cell

Γ_{ij} : Length of jth edge of ith cell

The ordinary differential equation at each cell is solved with a time-integration scheme.

Placement of variables

The conservative variables of the flow depth (h) and the flow rate (hu, hv) are stored at the cell centers.

The height of the flow bed (z) is stored and computed at the cell vertices (= cell nodes).

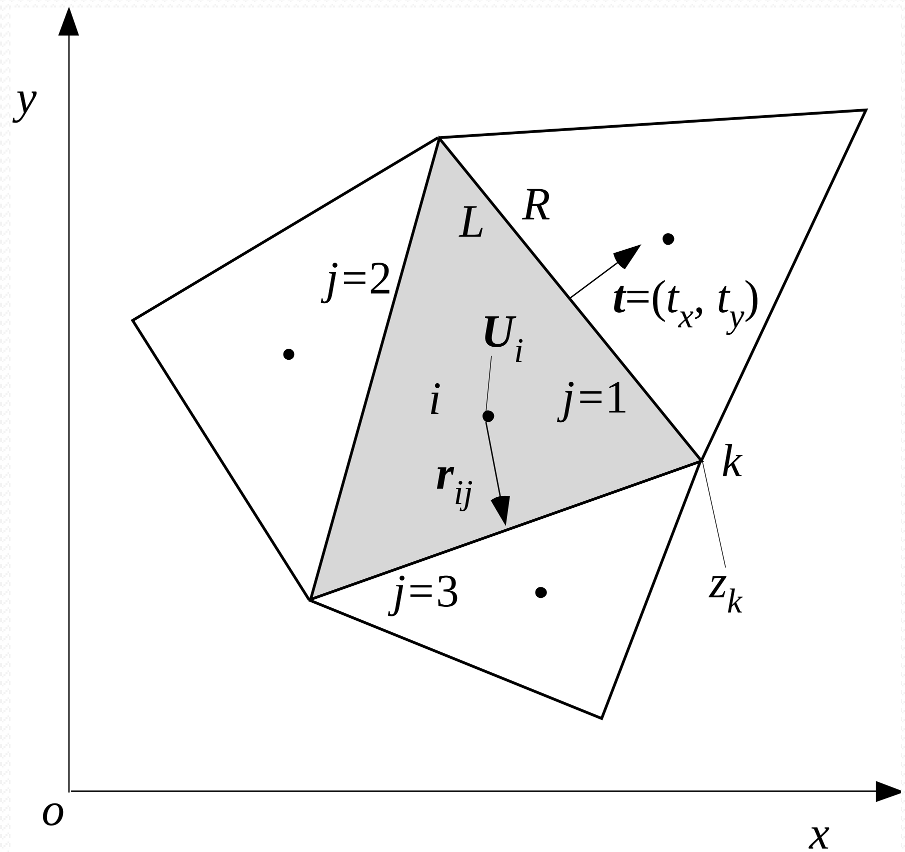

Computation and stabilization

1. The numerical method applied to this problem is MUSCL-type finite volume method, using an approximate Riemann solver with the implementation of a slope limiter and Surface Gradient Method (SGM).

"Riemann solver" means the computation of exact solutions for the intercell flux.

"Slope limiter" constrains the gradients of variables on cells for stable computation.

2. The change in flow bed height is simultaneously solved with the shallow water equations. TVD Runge-kutta scheme is used for the time integration .

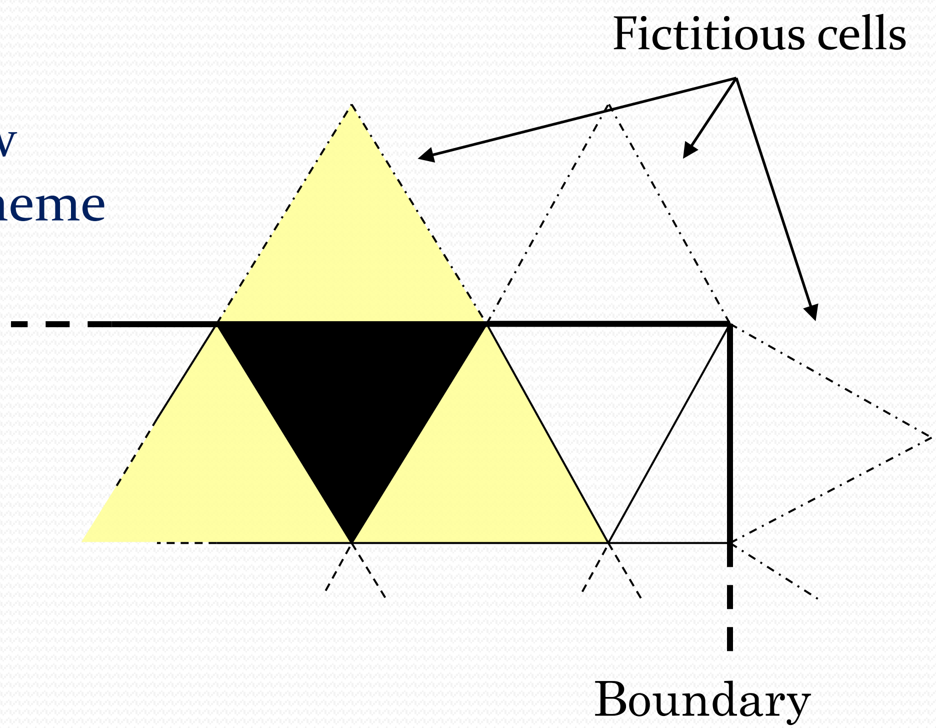

3. Fictitious cells were installed at the boundary to input natural boundary condition for water flow and to accurately compute the elevation change of the water bed

Treatment of source term & Time integration

$$\boxed{\frac{\partial \mathbf{U}}{\partial t}+\frac{\partial \mathbf{F}}{\partial x}+\frac{\partial \mathbf{G}}{\partial y}=\mathbf{S}}$$

$$\mathbf{U}=\begin{pmatrix} h \\ uh \\ vh \end{pmatrix} \quad \mathbf{F}=\begin{pmatrix} uh \\ u^2h+gh^2/2 \\ uvh \end{pmatrix} \quad \mathbf{G}=\begin{pmatrix} vh \\ uvh \\ v^2h+gh^2/2 \end{pmatrix}$$

$$\frac{\partial \mathbf{U}_i}{\partial t}=\boxed{-\frac{1}{A_i}\sum_{j=1}^{3}\mathbf{E}^*\cdot\mathbf{n}_{ij}\Delta\Gamma_{ij}+\mathbf{S}_i}$$

$$\mathbf{S}=\mathbf{S_o}+\mathbf{S_f}=\begin{pmatrix} 0 \\ ghS_{ox} \\ ghS_{oy} \end{pmatrix}+\begin{pmatrix} 0 \\ -ghS_{fx} \\ -ghS_{fy} \end{pmatrix}$$

$$\begin{cases} \dfrac{\partial \boldsymbol{U}_i}{\partial t}=\boldsymbol{S}_f & \text{Implicitly solved} \\[2ex] \dfrac{\partial \boldsymbol{U}_i}{\partial t}=-\dfrac{1}{A_i}\displaystyle\sum_{j=1}^{3}\boldsymbol{E}^*\cdot\boldsymbol{n}_{ij}\Delta\Gamma_{ij}+\boldsymbol{S}_0 \end{cases}$$

Explicitly solved

Third order TVD
Runge-Kutta Scheme

$$\boxed{\frac{\partial z}{\partial t}=\boxed{-\frac{E}{1-\lambda}}}$$

$$\boldsymbol{U}^{(1)}=\boldsymbol{U}^{n}+\Delta t\underline{L(z^{n},\boldsymbol{U}^{n})} \qquad z^{(1)}=z^{n}+\Delta t\underline{I(z^{n},\boldsymbol{U}^{n})}$$

$$\boldsymbol{U}^{(2)}=\frac{3}{4}\boldsymbol{U}^{n}+\frac{1}{4}\boldsymbol{U}^{(1)}+\frac{1}{4}\Delta t\underline{L(z^{(1)},\boldsymbol{U}^{(1)})} \qquad z^{(2)}=\frac{3}{4}z^{n}+\frac{1}{4}z^{(1)}+\frac{1}{4}\Delta t\underline{I(z^{(1)},\boldsymbol{U}^{(1)})}$$

$$\boldsymbol{U}^{n+1}=\frac{1}{3}\boldsymbol{U}^{n}+\frac{2}{3}\boldsymbol{U}^{(2)}+\frac{2}{3}\Delta t\underline{L(z^{(2)},\boldsymbol{U}^{(2)})} \qquad z^{n+1}=\frac{1}{3}z^{n}+\frac{2}{3}z^{(2)}+\frac{2}{3}\Delta t\underline{I(z^{(2)},\boldsymbol{U}^{(2)})}$$

Surface Gradient Method

The conservative variables are the flow depth (h) and the flow rates(hu, hv) and usually these variables are interpolated over cells. However, the SGM interpolates the height of water surface instead of the flow depth.

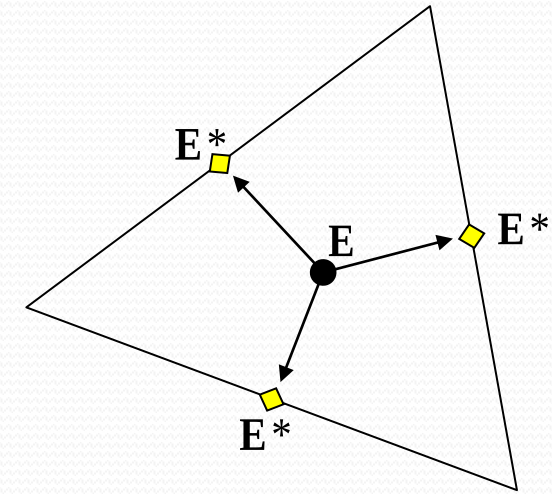

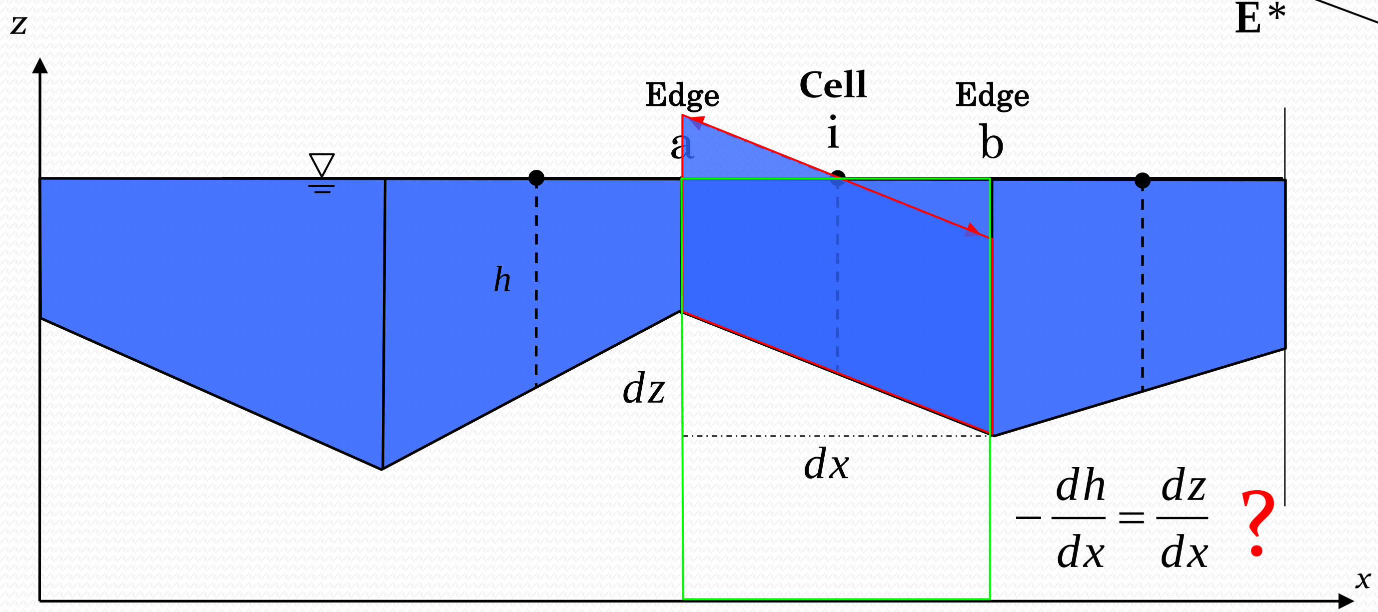

Zhou et al. (2001) : The surface gradient method for the treatment of source term in the shallow-water equations. *Journal of Computational Physics*, **168**,pp.1-25.

Surface Gradient Method (C-property)

$$\frac{\partial \mathbf{U}}{\partial t}+\frac{\partial \mathbf{F}}{\partial x}+\frac{\partial \mathbf{G}}{\partial y}=\mathbf{S}$$

$$\mathbf{U}=\begin{pmatrix} h \\ uh \\ vh \end{pmatrix} \quad \mathbf{F}=\begin{pmatrix} uh \\ u^2h+gh^2/2 \\ uvh \end{pmatrix} \quad \mathbf{G}=\begin{pmatrix} vh \\ uvh \\ v^2h+gh^2/2 \end{pmatrix}$$

$$\mathbf{S}=\mathbf{S_o}+\mathbf{S_f}=\begin{pmatrix} 0 \\ ghS_{ox} \\ ghS_{oy} \end{pmatrix}+\begin{pmatrix} 0 \\ -ghS_{fx} \\ -ghS_{fy} \end{pmatrix}$$

When the flow velocities are zero and the water level is constant;

$$\frac{\partial \boldsymbol{F}}{\partial x}+\frac{\partial \boldsymbol{G}}{\partial y}=\boldsymbol{S}_0$$

$$\boldsymbol{F}=\begin{pmatrix} 0 \\ gh^2/2 \\ 0 \end{pmatrix} \quad \boldsymbol{G}=\begin{pmatrix} 0 \\ 0 \\ gh^2/2 \end{pmatrix} \quad \boldsymbol{S}_o=\begin{pmatrix} 0 \\ -gh\partial z/\partial x \\ -gh\partial z/\partial y \end{pmatrix}$$

Flux term

$$g\frac{1}{2}\frac{\partial}{\partial x}(\eta-z)^2$$

$$=g\frac{1}{2}\frac{\partial}{\partial x}\left(\eta^2-2\eta z+z^2\right)$$

$$=g\left(-\eta\frac{\partial z}{\partial x}+\boxed{\frac{1}{2}\frac{\partial z^2}{\partial x}}\right)$$

Gravitational term

$$gh\frac{\partial z}{\partial x}=g(\eta-z)\frac{\partial z}{\partial x}$$

$$=g\eta\frac{\partial z}{\partial x}-\boxed{z\frac{\partial z}{\partial x}}$$

$$=g\eta\frac{\partial z}{\partial x}-\frac{1}{2}\frac{\partial z^2}{\partial x}$$

2-D simulation - examples -

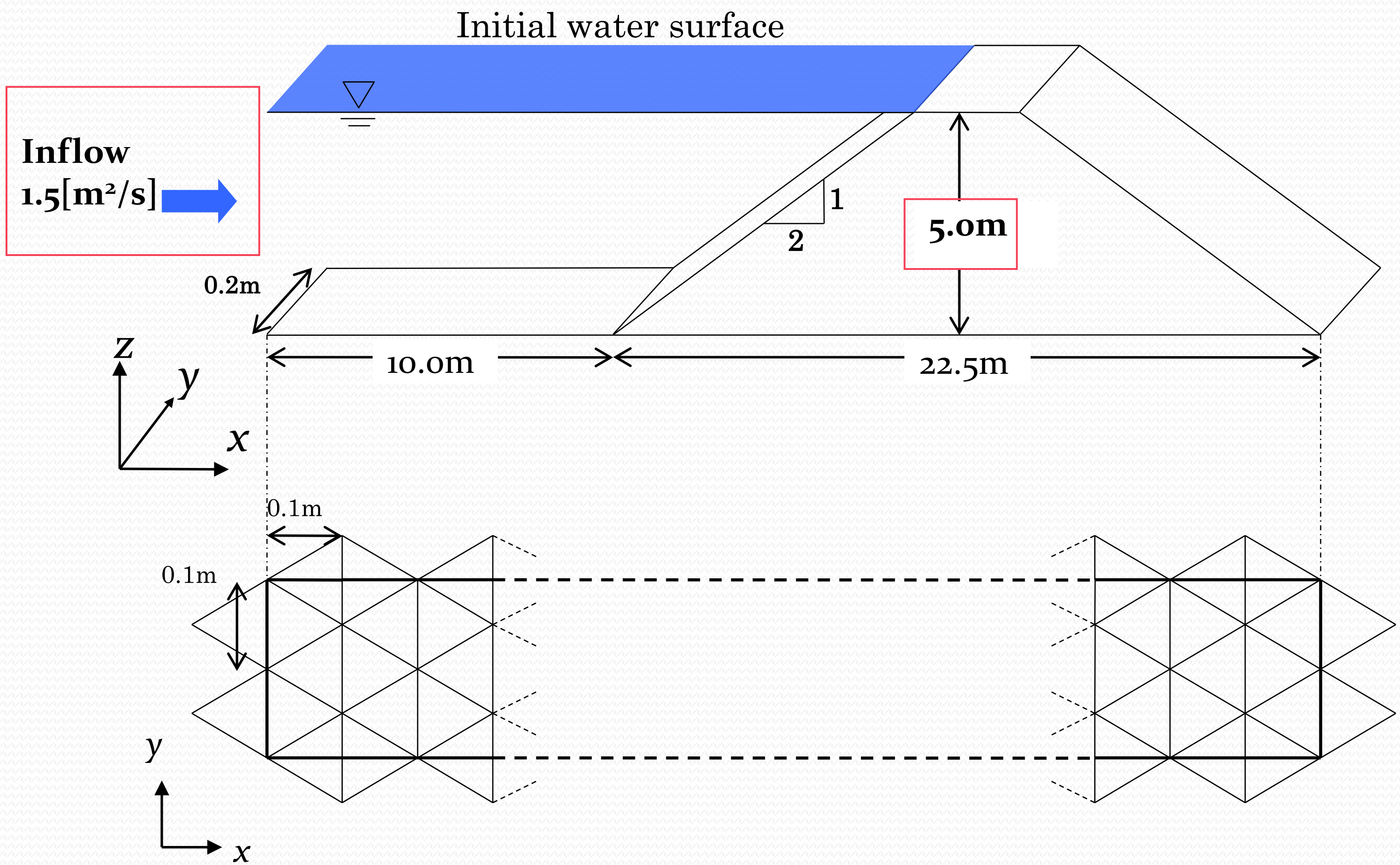

Calculation grids

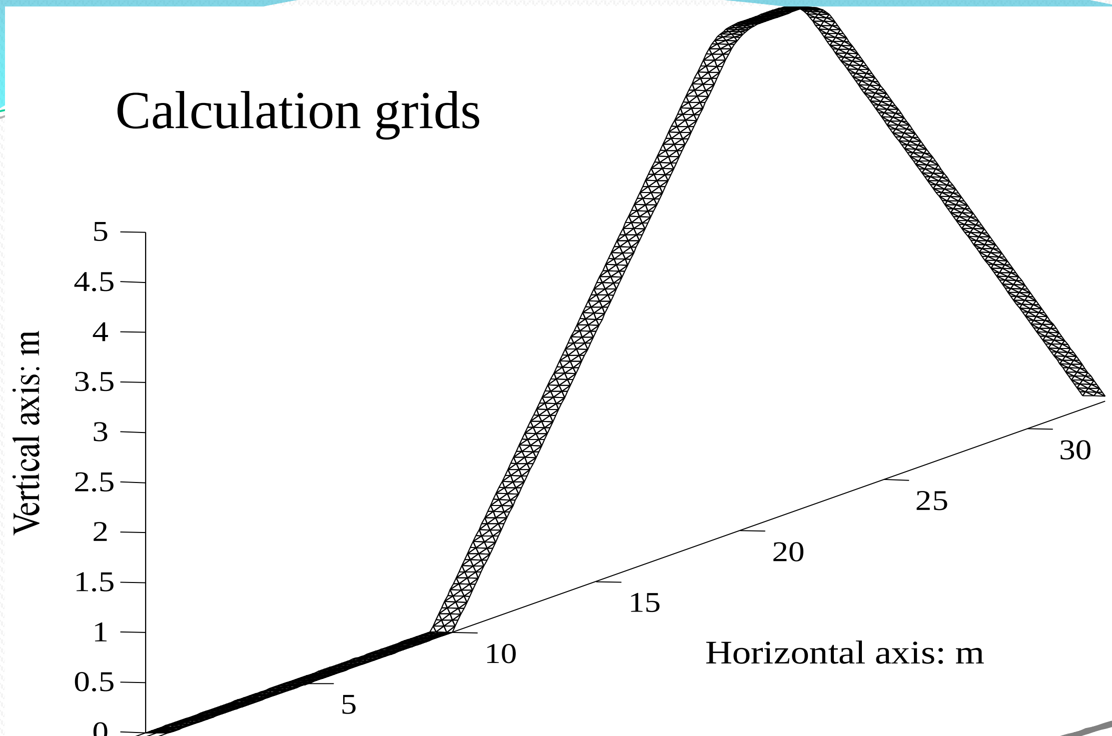

Flow rate=1.5 $m^3/s/m$

Manning's coefficient=0.019

Simulation result
(Embankment profiles)

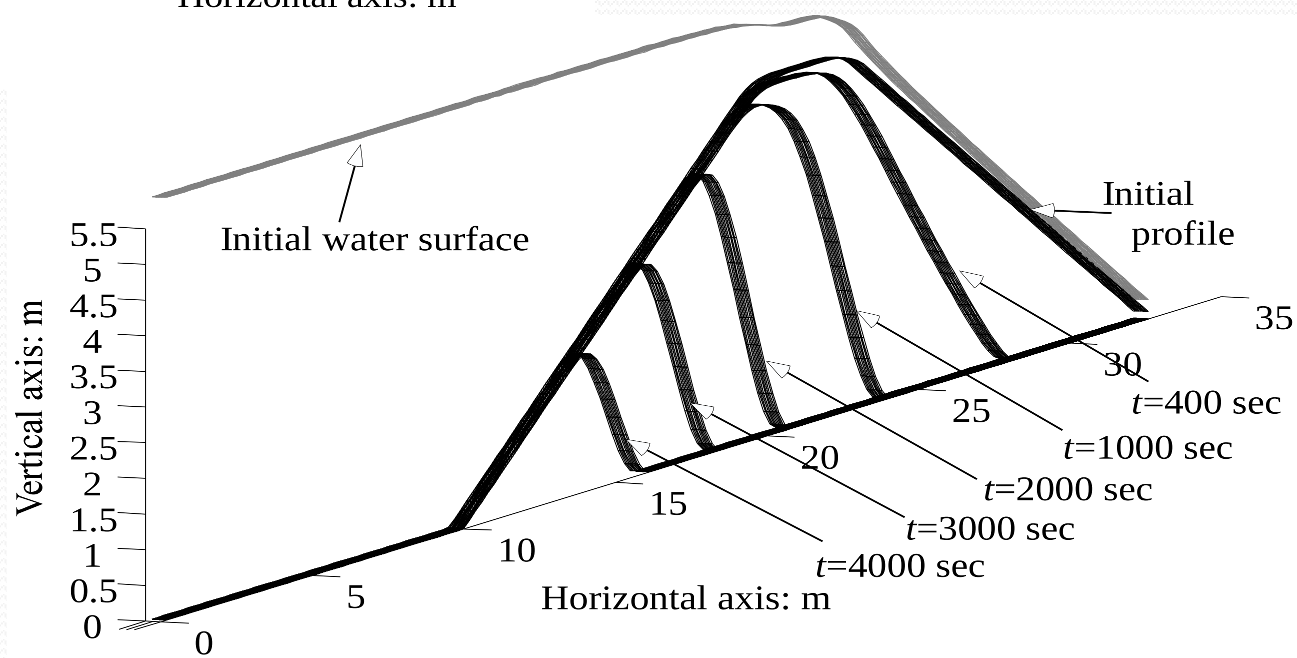

Verification

Input parameters:

Porosity=0.395, Critical shear stress (τ_c)=1.0Pa, α=7.84E-5 m/s/Pa$^{3/2}$

γ=1.5, Manning's coefficient=0.0168

Boundary conditions:

Inflow rate=0.021 m^3/s/m at the left side.

Free outfall boundary for the right side.

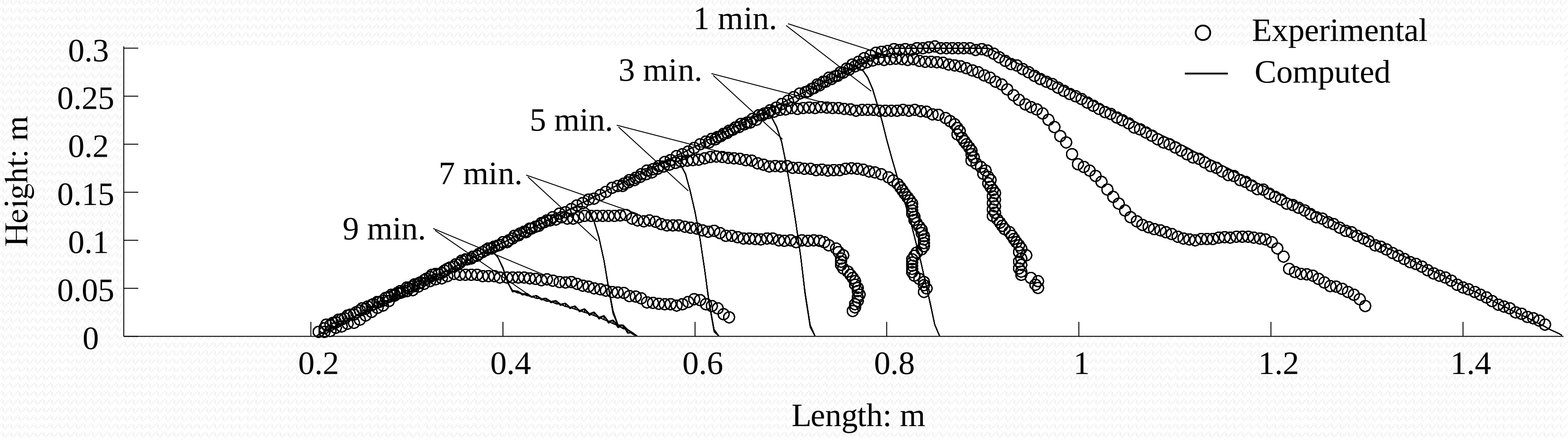

3-D simulation – settings -

A scar (initial disturbance) with the depth of 2 cm is given on the top of the embankment, which might induce the concentration of the overflow and erosion.

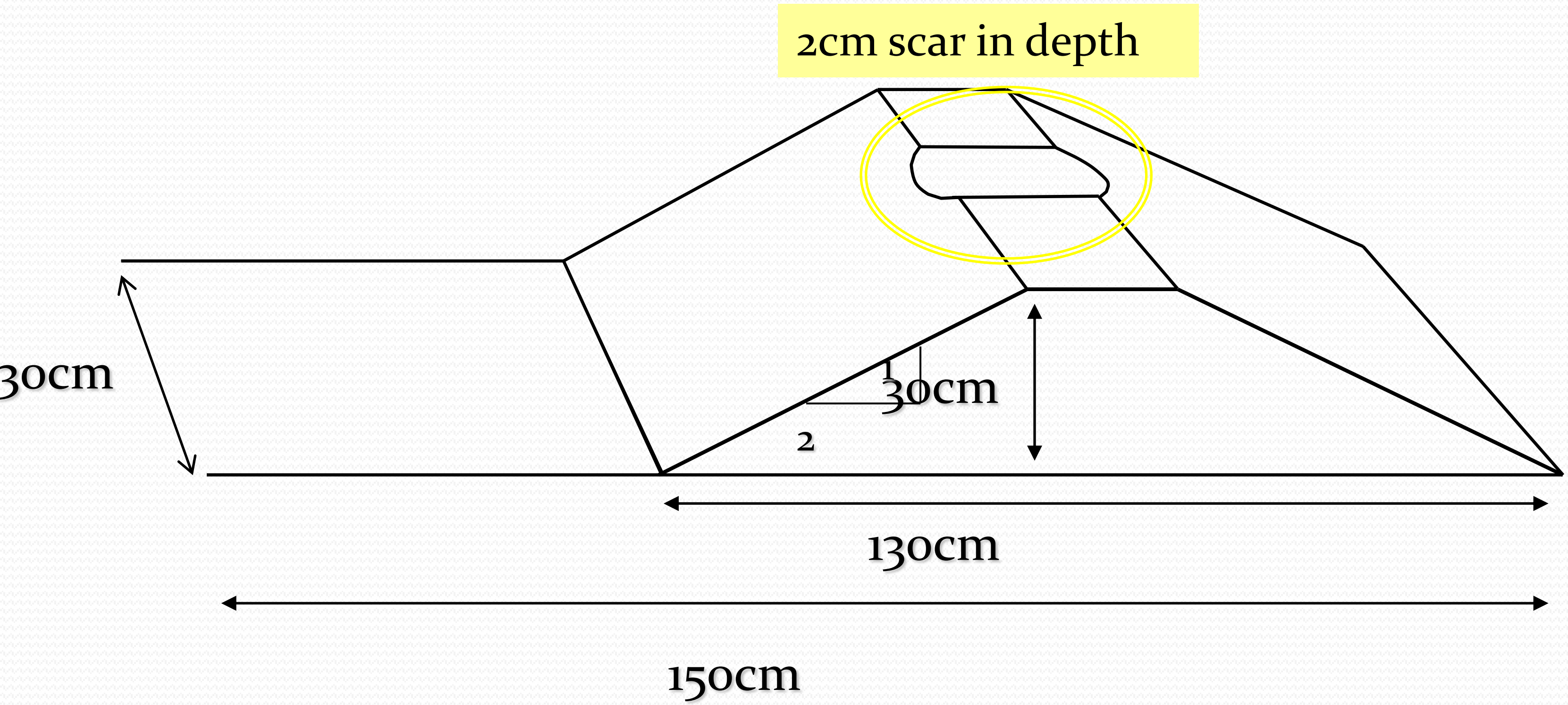

Concept on 3-D simulation

Input parameters:

Porosity=0.395, Critical shear stress (τ_c)=0.1Pa, α=8.42E-5 m/s/Pa$^{3/2}$

γ=1.5, Manning's coefficient=0.0158

Boundary conditions:

Inflow rate=0.0029 m^3/s/m at the left side.

Free outfall boundary for the right side.

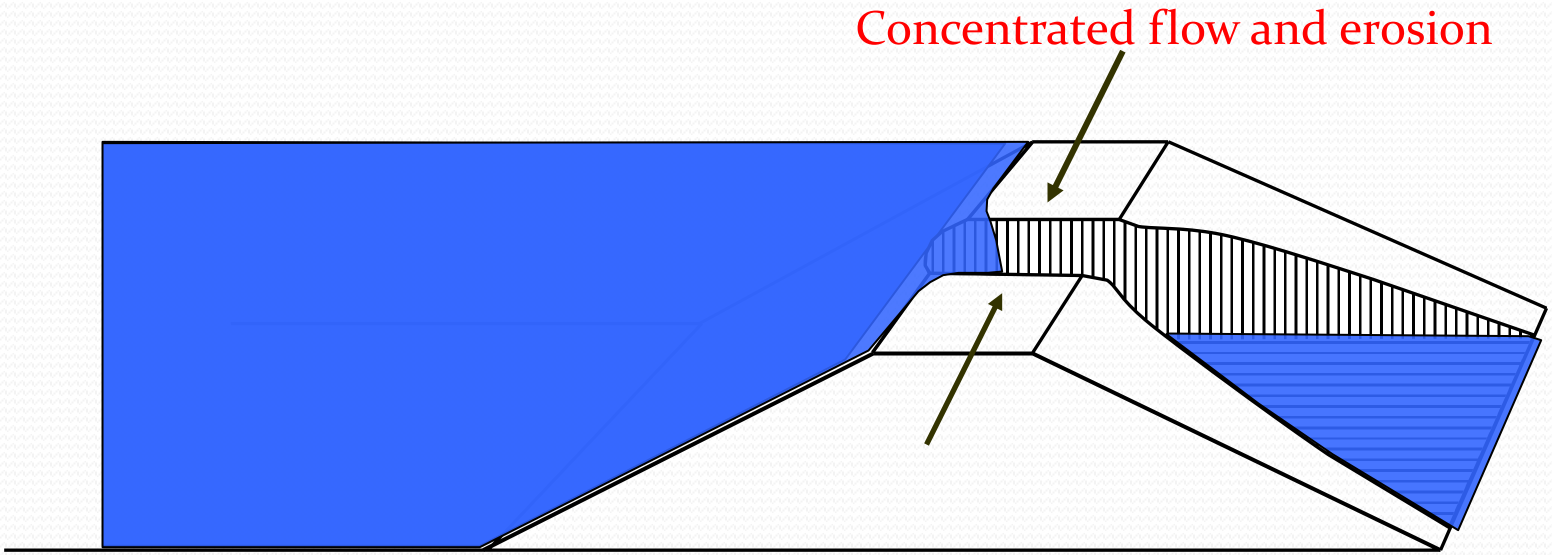

Numerical results

20 sec

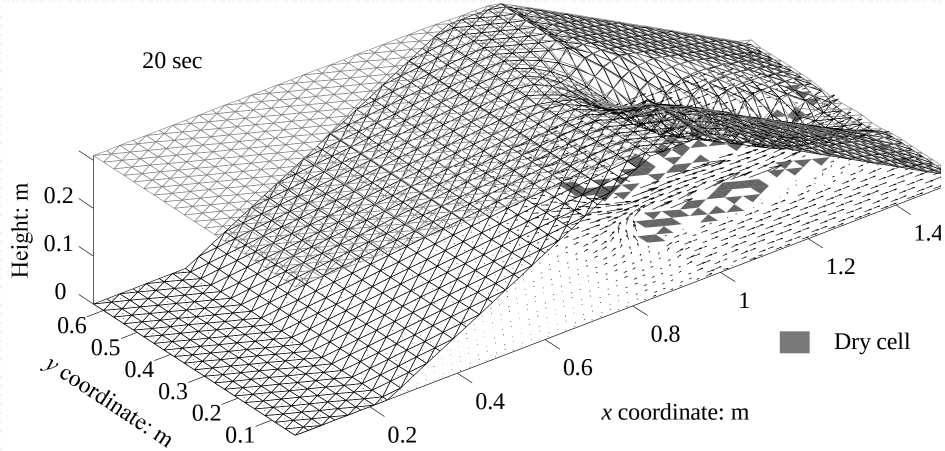

100 sec

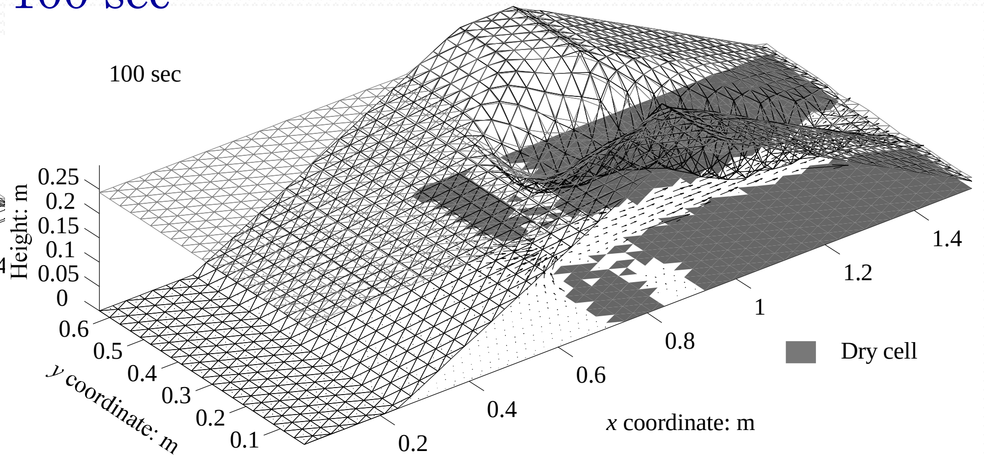

50 sec

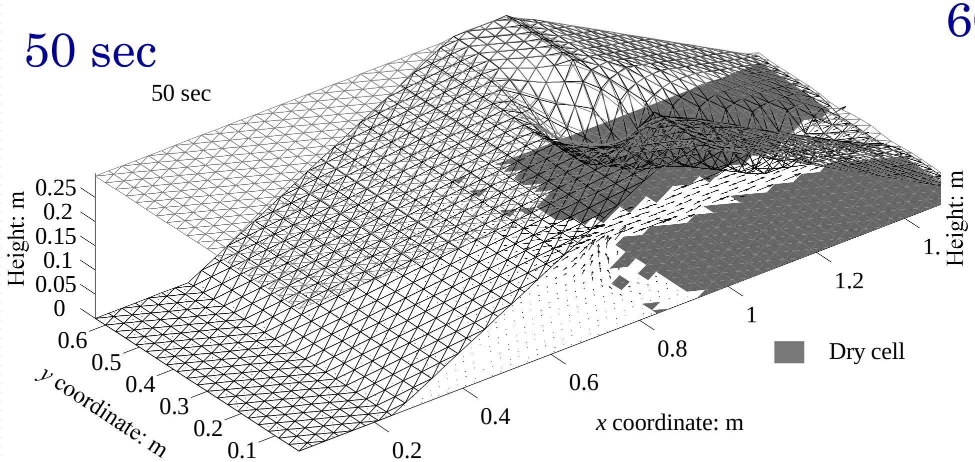

600 sec

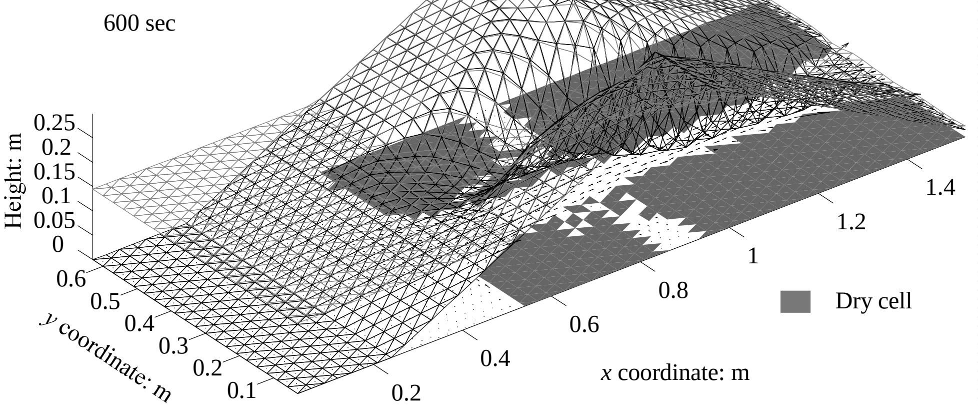

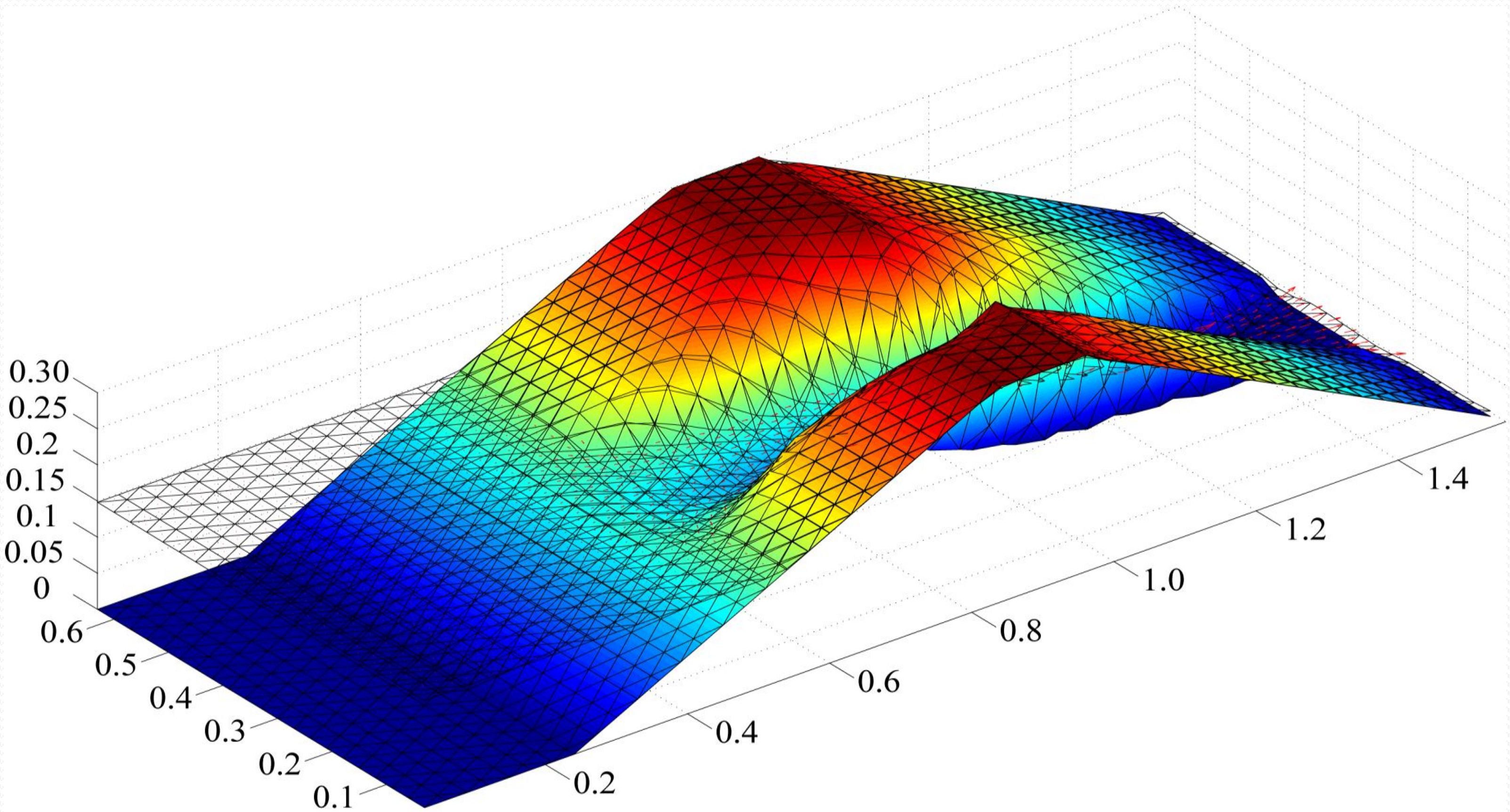
0.30
0.25
0.2
0.15
0.1
0.05
0
0.6
0.5
0.4
0.3
0.2
0.1
0.2
0.4
0.6
0.8
1.0
1.2
1.4

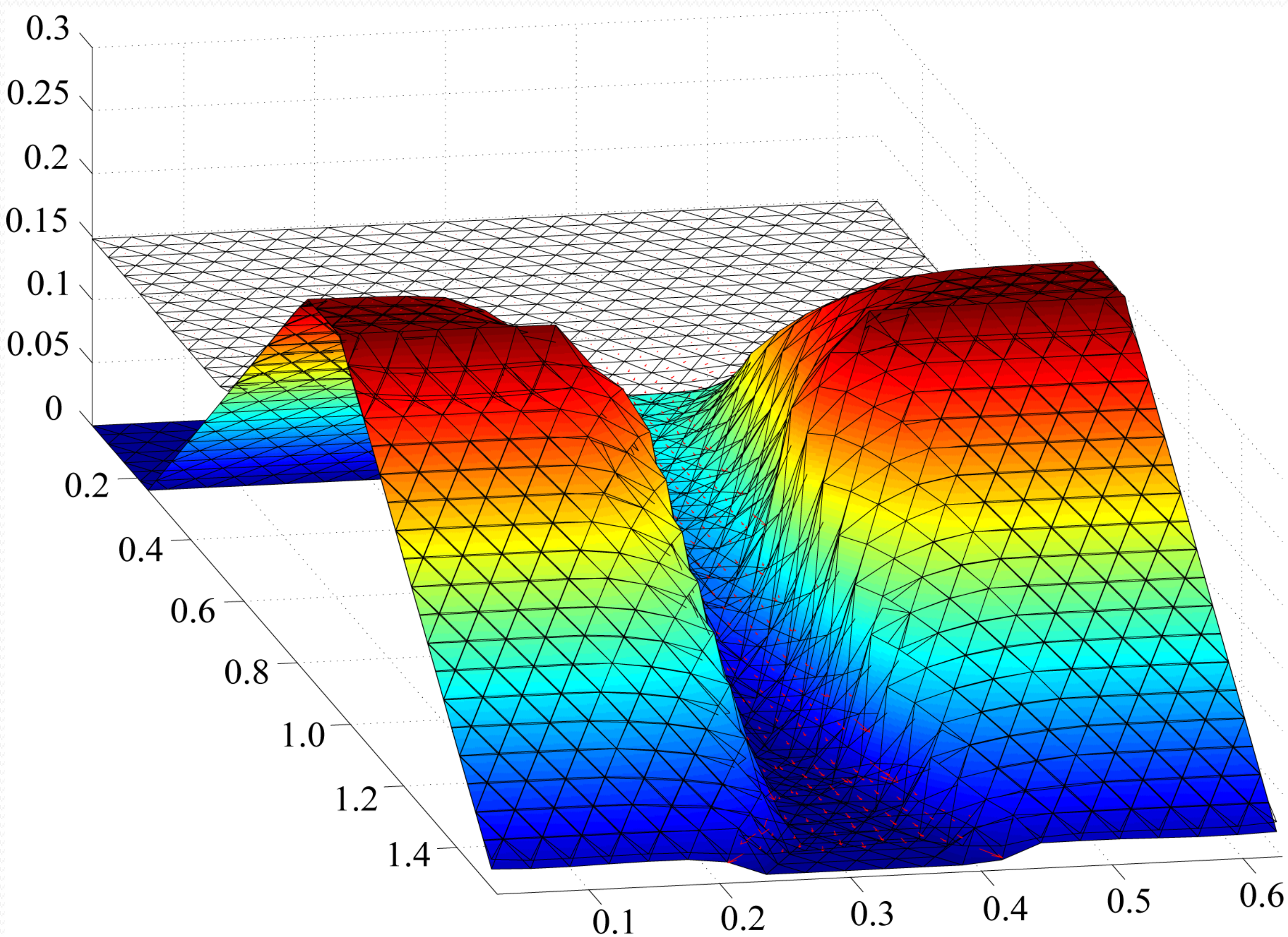

0.3
0.25
0.2
0.15
0.1
0.05
0
0.2
0.4
0.6
0.8
1.0
1.2
1.4
0.1
0.2
0.3
0.4
0.5
0.6

Summary

1. The numerical solution of 2D shallow water equations and the erosion rates of embankment material allow us to determine the profiles of embankments subjected to overflow erosion.

2.Surface Gradient Method is quite helpful when the complex geometry of flow beds is dealt with.(We must check "C-property" that makes sure the balance between the flux and gravitational terms under steady state)

3. 3-dimensional analysis is also possible by the proposed method. The next step is to verify and predict the width of the erosion channel and to try the large scale simulation.

Thank you for your attention !

Slope limiter

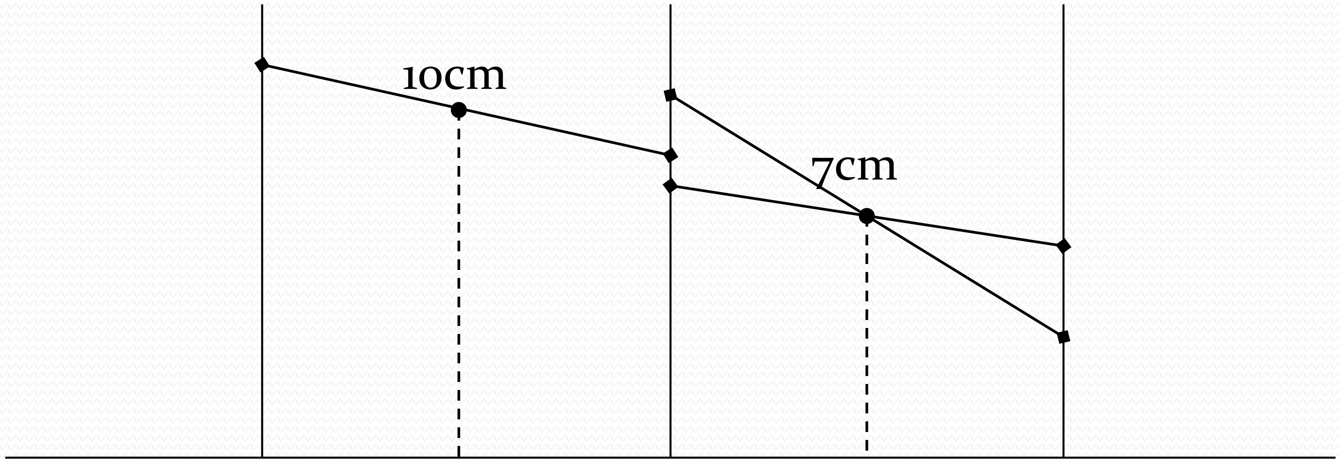

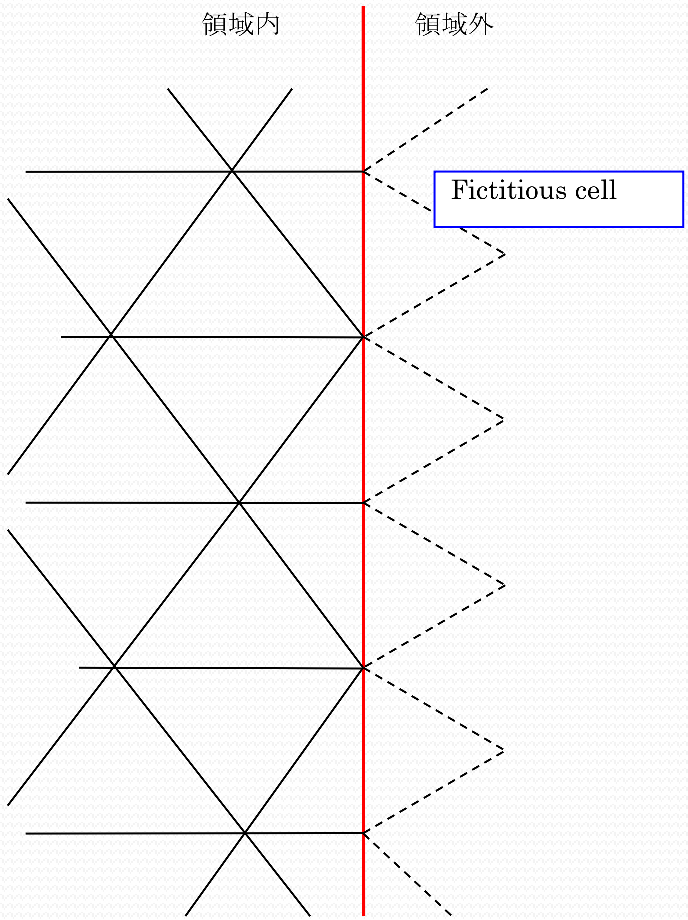

領域内
領域外
Fictitious cell

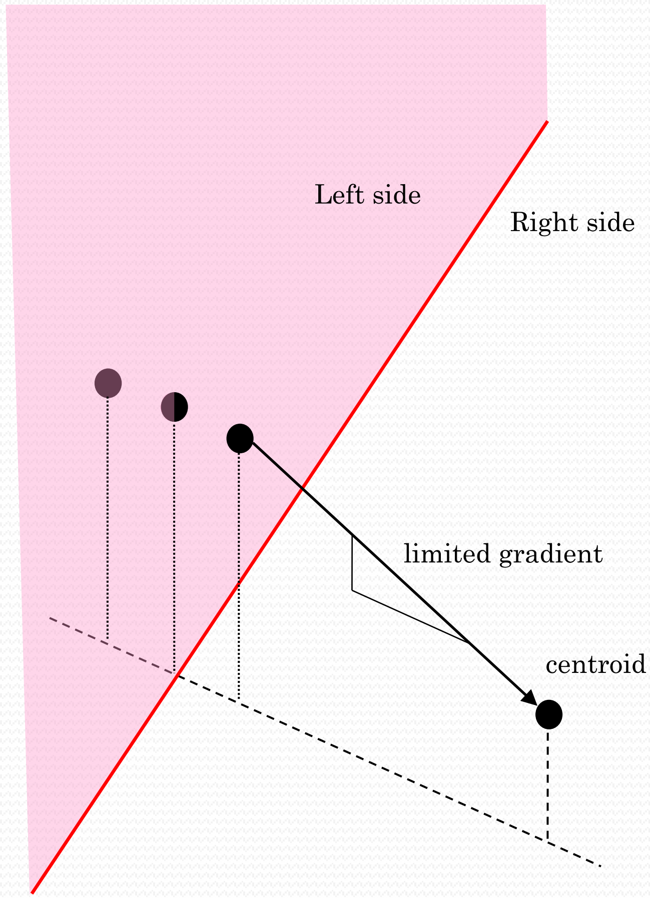

Left side
Right side
limited gradient
centroid

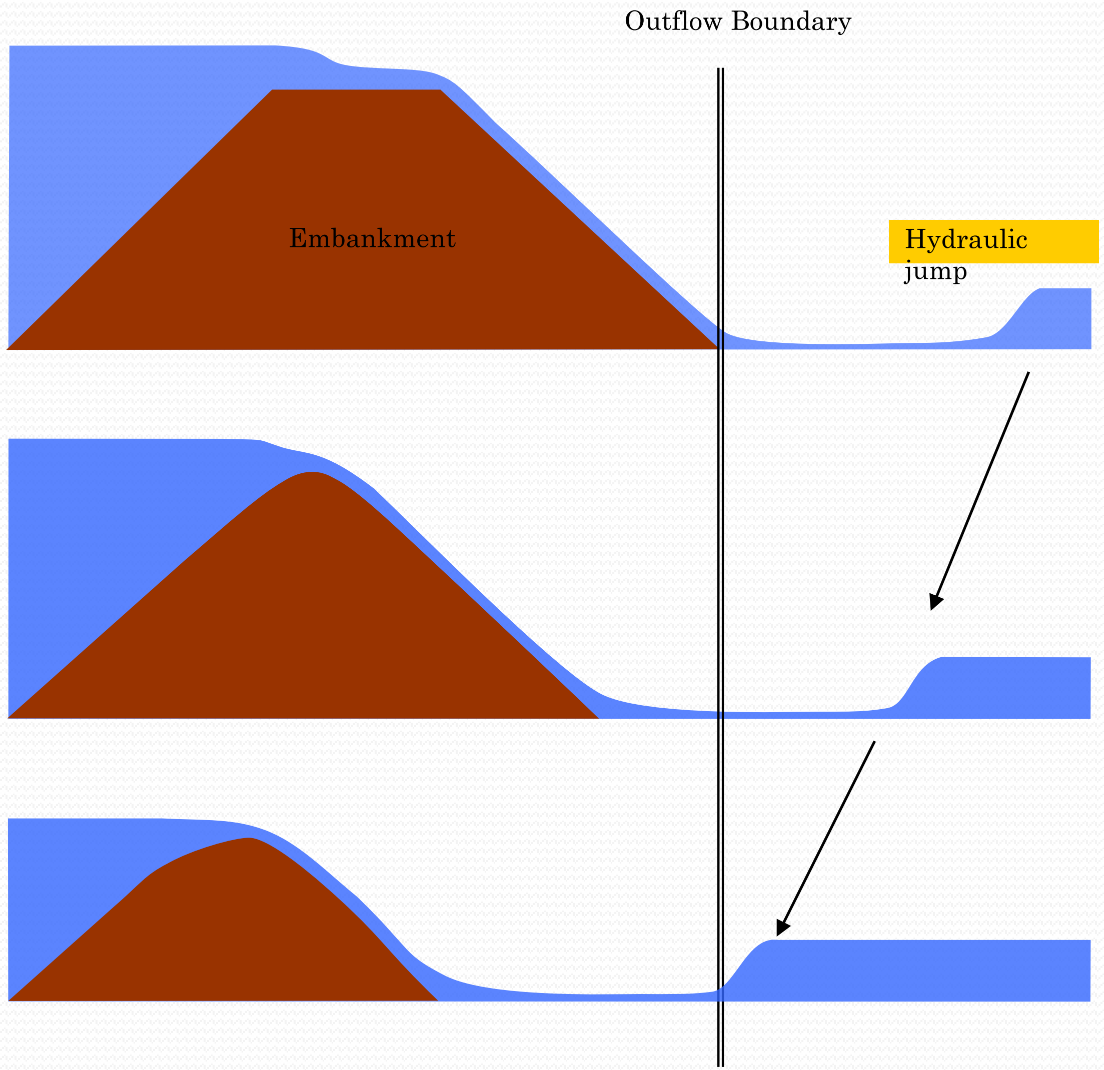

Outflow Boundary
Embankment
Hydraulic jump